SPATIALLY INTERPOLATED BEAMFORMING USING DISCRETE PROLATE SPHEROIDAL SEQUENCES

Matt Ruan, Leif W. Hanlen, Mark C. Reed

Australian National University & National ICT Australia

ABSTRACT

This paper presents a novel design method for a spatially interpolated beamformer. By separating the design of the physical antenna array and the digital signal processors, we remove the restriction on the half-wavelength spacing requirement of a uniform linear array to achieve higher efficiency. To be more realistic, however, we fix the element positions regardless of the steering angles. The maximum energy concentration properties of discrete prolate spheroidal sequences are exploited to optimize the weighting coefficients and filtering window. Two examples are given to demonstrate the high flexibility, low computational complexity, and non compromised performance of the proposed beamformer.

1. INTRODUCTION

Spatial diversity is one of the most important resources to be exploited by future wireless communication systems, and the smart antenna based space division multiplexing technology is very useful [1][2].

As early as 1948, the Dolph-Chebyshev array was introduced by [3] and became one of the most widely used spatial beamforming methods. With the development of digital signal processing technologies, it becomes easier and less expensive to beamform with over-sampling and some other digital processing techniques in time or frequency domain[4]. However, as the spatial filtering effects of the antenna arrays are not exploited by those methods, they often require more computational resources than actually needed.

Spatially interpolated beamforming can be seen as a compromise between the spatial and temporal approaches mentioned above, and was introduced by [2]. That paper proposed to expand the element interval of a traditional Dolph-Chebyshev array by N times, and use a Chebyshev digital window to eliminate the aliasing main lobes resulted from the expansion. This way, with only a limited number of real sensors, one can approach the performance of a much larger antenna array. If a certain range of steering angles are to be supported, the method of [2] must change the interpolation point number, or equivalently, the interval of antenna elements, which is not feasible for many practical systems. Our method overcomes that problem by maximizing the antenna element interval as far as allowed by the steering angles, and using digital signal processing to suppress the aliasing main lobes. Thus, one fixed sensor array can support multiple steering angles as long as they are within the predefined angular region. The works of [2] followed traditional design of Chebyshev array and used Chebyshev digital windowing. Under the settings of spatially interpolated beamforming, where the main lobe shaping and side lobe suppressing are separately achieved by physical array and digital filtering, we propose to use discrete prolate spheroidal sequences (DPSS) [5] to take advantage of its maximum energy concentration property.

In this paper, we only discuss spatially interpolated beamformers based on uniform linear arrays (ULA), and they can be easily extended to two-dimensional uniform arrays.

2. SYSTEM MODEL AND DENOTATION

A diagram of the proposed far-field beamformer is shown in Fig. 1. The physical part of the beamformer is a classical ULA comprising M_e evenly distributed isotropic sensors fixed at interval d_e. We assume M_e is given, d_e is to be optimized for the whole range of steering angles, and neither can be changed on the fly. The fields on the sensors are [6]

$$\boldsymbol{F}(r,\theta) = F_0(r)\,\Omega_{M_e}(-\frac{2\pi}{\lambda}d_e\cos(\theta)) \qquad (1)$$

where $F_0(r)$ is the field on the first element of the array, $\Omega_M(t) = [1, e^{\iota t}, \cdots, e^{\iota(M-1)t}]$, $\iota = \sqrt{-1}$, λ is the wavelength of the signal, θ is the direction of arrival (DOA), and r is the distance between the transmitter and receiver.

The digital part of the beamformer is depicted in Fig. 1. The digital signal processor performs complex rotation of the field vector $\boldsymbol{F}(r,\theta)$ with $\Omega_{M_e}(\frac{2\pi}{\lambda}\frac{d_e}{N}\cos(\theta_0))$, and shapes the main lobe of angular response with a real coefficient vector $\boldsymbol{w}$. The $\mathcal{P}_N$ box shown in Fig. 1 symbolizes the interpolation operation, which just simply inserts $N-1$ zeros between every two entries of the input vector. The interpolated sequence is filtered by a M_w-tap digital window $\boldsymbol{h}$ to produce a $K = M_w + N(M_e-1)$ long vector, the summation of which

The authors are with the National ICT Australia and affiliated with the Australian National University. National ICT Australia is funded through the Australian Governments Backing Australia's Ability initiative and in part through the Australian Research Council. The email addresses are matt.ruan@rsise.anu.edu.au, {leif.hanlen, mark.reed}@nicta.com.au

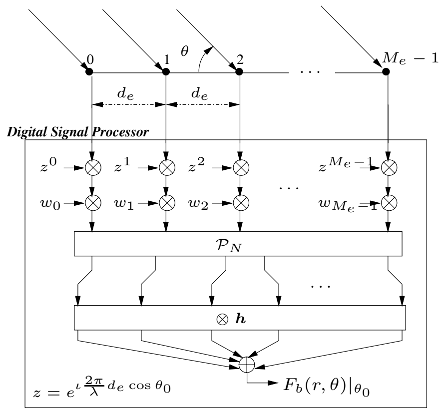

Fig. 1. Diagram of the proposed spatially interpolated beamformer

becomes the output of the beamformer for given steering angle θ_0, which is denoted by $F_b(r,\theta)|_{\theta_0}$.

Following [2, Eqn.(6)], we can write [1]

$$F_a(\theta) \triangleq \frac{F_b(r,\theta)}{F_0(r)} = F_e(\theta)F_h(\theta) \tag{2}$$

where

$$F_e(\theta) = \boldsymbol{w}^T \Omega_{M_e}(-d_e\varphi(\theta,\theta_0)) \tag{3}$$

$$F_h(\theta) = \boldsymbol{h}^T \Omega_{M_w}(-\frac{d_e}{N}\varphi(\theta,\theta_0)) \tag{4}$$

$$\varphi(\theta,\theta_0) \triangleq \frac{2\pi}{\lambda}(\cos\theta - \cos\theta_0) \tag{5}$$

$F_e(\theta)$ and $F_h(\theta)$ are the angular response of the analog and digital parts of the beamformer respectively. $\varphi(\theta,\theta_0)$ is a normalized measure of the direction of arrival θ in respect to the steering angle θ_0 and wavelength λ.

3. THE METHOD

For a fixed number of sensors, our strategy is to maximize interval d_e, then use the digital signal processors to suppress the aliasing main lobes and achieve the desirable performance.

Define the range of the steering angles to be $\mathbb{S}_1 = [\theta_z, \pi - \theta_z]$, where $0 < \theta_z \leq \frac{\pi}{2}$. The null power angle $\Delta\theta$ is defined such that for all $\theta \in (0, \theta_0 - \Delta\theta] \cup [\theta_0 + \Delta\theta, \pi)$, $20(\log_{10}|F_a(\theta)| - \log_{10}|F_a(\theta_0)|) < \eta$, where η is the desirable side lobe level. The half power angle $\Delta\theta_h$ is defined such that for all $\theta \in (0, \theta_0 - \Delta\theta_h] \cup [\theta_0 + \Delta\theta_h, \pi)$, $20(\log_{10}|F_a(\theta)| - \log_{10}|F_a(\theta_0)|) < -3$. The set of parameters $\{\theta_z, \Delta\theta, \Delta\theta_h, \eta\}$ specifies the beamformer.

[1] Throughout this work we utilize the assumptions of [2] with regard to the utilization of Eqn.(6) in their paper. Under certain circumstances the assumptions behind [2, Eqn.(6)] may not be realistic, as the operation may require an unreasonable apriori field constraint over the entire sampling region. We show the improvements that could be made upon the works of [2] rather than questioning their basic assumptions.

3.1. Element Interval and Weighting Optimization

Consider the optimization of the physical antenna array. For a given M_e, calculate the optimal interval d_e and weighting vector $\boldsymbol{w}$ in terms of maximum energy concentration.

Define $[\theta_c, \theta_d] \subseteq [\theta_0 - \Delta\theta, \theta_0 + \Delta\theta] \subseteq [\theta_a, \theta_b]$:

$$|\varphi(\theta_a,\theta_0)| = |\varphi(\theta_b,\theta_0)| = \Psi(\theta_0,\Delta\theta)$$
$$|\varphi(\theta_c,\theta_0)| = |\varphi(\theta_d,\theta_0)| = \psi(\theta_0,\Delta\theta)$$

where $\Psi(\theta_0,\Delta\theta)$ and $\psi(\theta_0,\Delta\theta)$ are the larger and smaller values of $|\varphi(\theta_0 - \Delta\theta, \theta_0)|$ and $|\varphi(\theta_0 + \Delta\theta, \theta_0)|$ respectively.

To put $[\theta_a, \theta_b]$ inside the main lobe, the sensor interval d_e should not exceed the maximal value d_e^{max}, which can be calculated by

$$d_e^{max} = \begin{cases} \frac{\lambda}{4\sin\frac{\Delta\theta}{2}} & 0 < \theta_z \leq \frac{\pi - \Delta\theta}{2} \\ \frac{\lambda}{4\sin\frac{\Delta\theta}{2}\sin(\theta_z + \frac{\Delta\theta}{2})} & \frac{\pi-\Delta\theta}{2} < \theta_z \leq \frac{\pi}{2} \end{cases} \tag{6}$$

As $[\theta_c, \theta_d] \subseteq [\theta_a, \theta_b]$, for all $d_e \leq d_e^{max}$, $[\theta_c, \theta_d]$ should also in main lobe. Evaluate the energy concentrated by the real antenna array into $[\theta_c, \theta_d]$ as follows.

$$P_e(\theta_c,\theta_d) \triangleq \int_{\varphi(\theta_d,\theta_0)}^{\varphi(\theta_c,\theta_0)} |F_e(\varphi^{-1}(u,\theta_0))|^2 du$$
$$= \sum_{k=0}^{M_e-1}\sum_{j=0}^{M_e-1} w_k w_j \int_{-\Delta u_e}^{\Delta u_e} e^{-\iota u d_e (k-j)} du = \frac{1}{d_e}\boldsymbol{w}^T \boldsymbol{G}\, \boldsymbol{w}$$

where $\boldsymbol{G}$ is a symmetric $M_e \times M_e$ matrix whose entries are

$$g_{k,j}(W_e) \triangleq \frac{\sin\left(2\pi W_e(k-j)\right)}{k-j},\ k,j \in [0, M_e - 1] \tag{7}$$

and $W_e \triangleq \frac{1}{2\pi} d_e \Delta u_e$, which follows [5] and [7] for DPSS. Under the constrain $\boldsymbol{w}^T\boldsymbol{w} = 1$, the optimal sequence $\boldsymbol{w}$ is the eigenvector corresponding to the maximal eigenvalue of $\boldsymbol{G}$, which is a DPSS [5] [7].

The prolate spheroidal wave functions have the property of maximum energy concentration in both time and frequency domain; and [5] extended that result to the discrete case, giving the relationship between the parameters for continuous wave functions and DPSS. In our case,

$$c_e = \pi M_e W_e = \frac{1}{2} M_e d_e \Delta u_e \tag{8}$$

where c_e is the benchmark for energy concentration. The work of [5] pointed out that for a small positive W_e, and large $M_e \geq \lfloor \frac{c_e}{\pi W_e} \rfloor$, the eigenvalue corresponding to the DPSS defined by M_e and W_e is approximately the same as the prolate wave function defined by c_e that can be calculated by Eqn.(8).

We define c_e^{min} as the minimal value of c_e for satisfactory main lobe shaping, the corresponding minimal number of physical sensors M_e^{min} can be calculated by

$$M_e^{min} = \left\lceil \frac{2\, c_e^{min}}{d_e^{max}\psi(\theta_z,\Delta\theta)} \right\rceil = \left\lceil \frac{2\, c_e^{min}}{\pi\sin(\theta_z - \frac{\Delta\theta}{2})} \right\rceil \tag{9}$$

When $M_e < M_e^{min}$, there are insufficient antenna elements to shape the main lobe. It is best to have $d_e = d_e^{max}$ to maximize c_e and use the filtering window to further shape the main lobe. When $M_e \geq M_e^{min}$, a smaller $d_e = \frac{2\, c_{min}}{M_e \psi(\theta_z, \Delta\theta)}$ would reduce main lobe aliasing while still keep the desirable main lobe shape. This strategy can be written as

$$d_e = \min\left(d_e^{max}, \frac{2\, c_e^{min}}{M_e \psi(\theta_z, \Delta\theta)}\right) \tag{10}$$

where d_e is not necessarily an integer multiple of half wavelength, which usually yields better results than bounding the physical sensors to half-wavelength grids as assumed in [2].

3.2. Interpolation and Filter Optimization

This subsection considers optimizing the interpolation number N, the length of filtering window M_w, and the digital window coefficient $\boldsymbol{h}$ to suppress the aliasing main lobes resulting from expanded element intervals.

We design a digital filtering window to concentrate the energy within the angle range $[\phi_1, \phi_2]$. When $\frac{1}{2} M_e d_e \Delta u_e < c_e^{min}$, we set $\phi_1 = \theta_0 - \Delta\theta$, $\phi_2 = \theta_0 + \Delta\theta$, otherwise, we set $[\phi_1, \phi_2]$ to be the region between the first pair of null energy points to the left and right of the steering angle respectively.

Similar to the previous sub-section, we define $[\phi_c, \phi_d] \subseteq [\phi_1, \phi_2] \subseteq [\phi_a, \phi_b]$ such that

$$|\varphi(\phi_a, \theta_0)| = |\varphi(\phi_b, \theta_0)| = \max(|\varphi(\phi_1, \theta_0)|, |\varphi(\phi_2, \theta_0)|)$$

$$|\varphi(\phi_c, \theta_0)| = |\varphi(\phi_d, \theta_0)| = \min(|\varphi(\phi_1, \theta_0)|, |\varphi(\phi_2, \theta_0)|)$$

Define $d_w \triangleq \frac{1}{N}\, d_e$ chosen to avoid grating side lobes whose levels are above η to occur within $(0, \pi)$, so d_w satisfies

$$\max_{\theta \in [0,\pi]} |d_w \varphi(\theta, \theta_0)| \leq 2\pi - d_w \Delta v_w \tag{11}$$

or equivalently,

$$d_w \leq \frac{\lambda}{1 + |\cos\theta_0| + \frac{\lambda}{2\pi}\Delta v_w} \triangleq d_w^{max} \tag{12}$$

For all $d_w \leq d_w^{max}$,

$$d_w \Delta v_w \leq \frac{d_w}{2}(\Delta v_w + \max_{\theta \in [0,\pi]} |\varphi(\theta, \theta_0)|) \leq \pi \tag{13}$$

Therefore, $[\phi_a, \phi_b]$ is in the main lobe of $|F_h(\theta)|$, so is $[\phi_c, \phi_d]$. The energy concentration of the filtering window is

$$P_w(\phi_c, \phi_d) \triangleq \int_{\varphi(\phi_d)}^{\varphi(\phi_c)} |F_h(\varphi^{-1}(u))|^2 du$$

$$= \sum_{k=0}^{M_w-1} \sum_{j=0}^{M_w-1} h_k h_j \int_{-\Delta u_w}^{\Delta u_w} e^{-\iota u d_w (k-j)} du = \frac{1}{d_w} \boldsymbol{h}^T \boldsymbol{Q}\, \boldsymbol{h}$$

where $\boldsymbol{Q}$ is a symmetric $M_w \times M_w$ matrix whose entries are determined by the product of d_w and Δu_w. Under the constraint $\boldsymbol{h}^T \boldsymbol{h} = 1$, the optimal choice of $\boldsymbol{h}$ is the eigenvector corresponding to the maximal eigenvalue of $\boldsymbol{Q}$, which is a DPSS. Reference [5] shows for certain energy concentration, DPSS is the shortest sequence to achieve the desirable spectrum, which means the minimal value of M_w and the least computational complexity. Other advantages of DPSS as a family of digital windows were discussed in [7] and [8].

The minimal length of filtering window can be found by bisection search within the range from 1 to the M_w^{max}. It takes at most $\lceil \log_2 M_w^{max} \rceil$ trials to determine the value.

3.3. Summary of the Method

The proposed spatially interpolated beamforming method can be summarized as follows.

1. Determine the value of c_e^{min} required for main lobe shaping, and calculate d_e^{max} with Eqn.(6).
2. Obtain M_e^{min} from Eqn.(9), and d_e with Eqn.(10).
3. Compute $\boldsymbol{w}$ as a DPSS defined by M_e and W_e.
4. Find the filtering window null power angles ϕ_1 and ϕ_2, and compute the minimal interpolation point number $N = \left\lceil \frac{d_e}{d_w^{max}} \right\rceil$, where d_w^{max} is defined by Eqn.(12).
5. Find the minimal smoothing window length M_w that makes the resultant antenna array meet all the performance requirements. The filtering window $\boldsymbol{h}$ is a DPSS determined by M_w, d_w, the steering angle θ_0, and the null power angles ϕ_1 and ϕ_2.

4. DESIGN EXAMPLE AND NUMERICAL RESULTS

This section uses two examples to clarify the design procedures, and demonstrate the flexibility of the proposed method.

Example One uses the same specification as the example of [2], where a 5-element broadside beamformer with $\Delta\theta_h = 2.5°$, $\Delta\theta = 6°$, $\eta = -50dB$ is to be designed. We found $d_e^{max} = 4.7834\lambda$, $c_e^{min} = 2.56\pi$, $M_e^{min} = 6$, so $d_e = d_e^{max}$, $\boldsymbol{w} = [0.0625, 0.2500, 0.3750, 0.2500, 0.0625]^T$. We set $\phi_1 = 84°$, $\phi_2 = 96°$, and computed $N = 6$, $d_w = 0.7972\lambda$. The minimum length of DPSS window is 24. In [2], it shows the Chebyshev Array Chebyshev Window (CACW) beamformer needs 9 interpolation points and a 68-tap digital window to meet the same requirements. Fig. 2 shows the performance of both resultant beamformers. For other antenna sensor numbers, the reduced interpolation point number N and digital window length M_w are listed in Table 1.

In Example Two, one fixed array of $M_e = 6$ antenna sensors is to support steering angles between $30°$ and $150°$. First,

Table 1. Complexity Reduction Compared to [2, Table I]

M_e	20	15	11	9	7	6	5
Reduction in N	1	1	2	2	3	3	3
Reduction in M_w	5	8	14	18	29	34	44

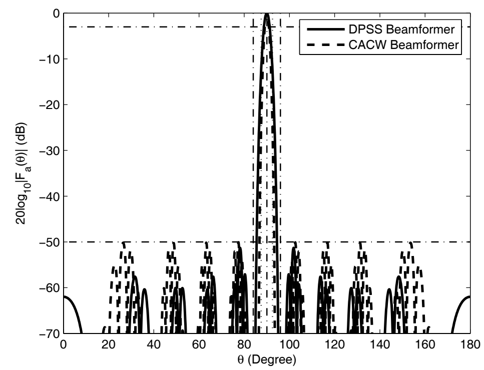

Fig. 2. Example One: Broadside ULA with DPSS spatial beamforming and Comparison with Chebyshev Array Chebyshev Window (CACW) Spatial Beamformer proposed by [2]

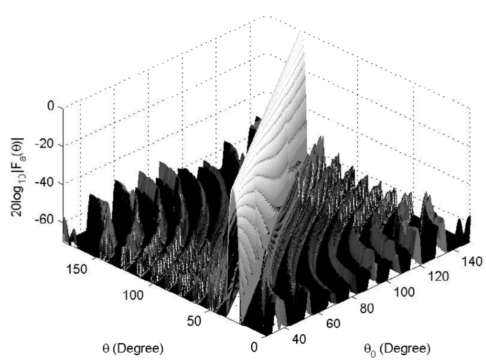

Fig. 3. Example Two: Fixed ULA with DPSS spatial beamforming supports the steering angles range from $30°$ to $150°$

we calculated $c_e^{min} = 2.56\pi$, $d_e^{max} = 4.7768\lambda$. When steering at $30°$ or $150°$, we found $M_e^{min} = 24$, so it would be better to place the sensors at the maximum interval ($d_e = d_e^{max}$) to achieve best main lobe shaping. Fig. 3 shows the performance of the proposed beamformer with steering angles stepping from $30°$ to $150°$ at $1°$ interval. On average it took 5.5 bisection searches for the minimal lengthes of filtering windows, which ranged from 24 to 73. For the 6-element array, the main lobe can be properly shaped when the steering angle is within $55.4°$ to $124.6°$; otherwise, for steering angles out of that region, further main lobe shaping by the digital filter is needed. This example demonstrates the high flexibility and non-compromised performance of the proposed beamforming method.

5. CONCLUSIONS

The spatially interpolated beamformer we proposed uses a standard ULA and a digital filtering window to achieve desirable main lobe shape and required side lobe levels for given steering angles. Using the method, we systematically and jointly optimize the physical and digital parts of the beamformer, we can thus efficiently fulfill the desirable performance with a limited number of physical antenna sensors. The low complexity and high flexibility of the proposed spatially interpolated beamformer could be used for next generation spatial division wireless communication systems.

6. REFERENCES

[1] L.C. Godara, "Applications of antenna arrays to mobile communications. I. Performance improvement, feasibility, and system considerations," *Proceedings of IEEE*, vol. 85, pp. 1031–1060, July 1997.

[2] Tuan Do-Hong and Peter Russer, "A new design method for digital beamforming using spatial interpolation," *IEEE Antennas and Wireless Propagation Letters*, vol. 2, pp. 177–181, 2003.

[3] C. L. Dolph, "A current distribution for broadside arrays which optimizes the relationship between beamwidth and side lobe level," *Proc. IRE*, vol. 34, pp. 335–348, 1946.

[4] Ronald A. Mucci, "A comparison of efficient beamforming algorithms," *IEEE Trans. Acoust. Speech Sig. Proc.*, vol. 32, no. 3, pp. 548–558, June 1984.

[5] D. Slepian, "Prolate spheroidal wave functions, Fourier analysis and uncertainty - V: the discrete case," *Bell System Technical Journal*, vol. 57, no. 5, pp. 1371–1430, May.-Jun. 1978.

[6] D. H. Werner, D. Mulyantini, and P. L. Werner, "Closed-form representation for directivity of nonuniformly spaced linear arrays with arbitrary element patterns," *Electronics Letters*, vol. 35, no. 25, pp. 2155–2157, December 1999.

[7] S. Bilbao T. Verma and T.H.Y. Meng, "The digital prolate spheroidal window," in *Proc. IEEE Int. Conf. Acoust., Speech, Signal Processing, ICASSP'1996*, Orlando, Florida, May 1996, vol. 3, pp. 1351–1354.

[8] J. K. Breakall John D. Mathews and Georg K. Karawas, "The discrete prolate speroidal filter as a digital signal processing tool," *IEEE Trans. Acoust. Speech Sig. Proc.*, vol. 33, pp. 1471–1478, Dec. 1985.